JOURNAL OF VIROLOGY, May 2010, p. 4912–4922 Vol. 84, No. 10
0022-538X/10/$12.00 doi:10.1128/JVI.02486-09

Innate Immune Responses and Permissiveness to Ranavirus Infection of Peritoneal Leukocytes in the Frog *Xenopus laevis*▽

Heidi D. Morales,[2]† Lara Abramowitz,[3] Jacqueline Gertz,[1] Jessica Sowa,[1] Ashley Vogel,[1] and Jacques Robert[1]*

Department of Microbiology and Immunology, University of Rochester Medical Center, Rochester, New York 14642[1]; Department of Neurobiology, Dana Farber Cancer Institute, Harvard Medical School, Boston, Massachusetts 02115[2]; and Department of Genetics, University of Pennsylvania Medical Center, Philadelphia, Pennsylvania[3]

Received 25 November 2009/Accepted 23 February 2010

Ranaviruses such as frog virus 3 ([FV3] family *Iridoviridae*) are increasingly prevalent pathogens that infect reptiles, amphibians, and fish worldwide. Whereas studies in the frog *Xenopus laevis* have revealed the critical involvement of CD8 T-cell and antibody responses in host resistance to FV3, little is known about the role played by innate immunity to infection with this virus. We have investigated the occurrence, composition, activation status, and permissiveness to infection of peritoneal leukocytes (PLs) in *Xenopus* adults during FV3 infection by microscopy, flow cytometry, and reverse transcription-PCR. The total number of PLs and the relative fraction of activated mononucleated macrophage-like cells significantly increase as early as 1 day postinfection (dpi), followed by NK cells at 3 dpi, before the peak of the T-cell response at 6 dpi. FV3 infection also induces a rapid upregulation of proinflammatory genes including arginase 1, interleukin-1β, and tumor necrosis factor alpha. Although PLs are susceptible to FV3 infection, as evidenced by apoptotic cells, active FV3 transcription, and the detection of viral particles by electron microscopy, the infection is weaker (fewer infectious particles), more transitory, and involves a smaller fraction (less than 1%) of PLs than the kidney, the main site of infection. However, viral DNA remains detectable in PLs for at least 3 weeks postinfection, past the point of viral clearance observed in the kidneys. This suggests that although PLs are actively involved in anti-FV3 immune responses, some of these cells can be permissive and harbor quiescent, asymptomatic FV3.

Ranaviruses (RVs), of the family *Iridoviridae*, are large (165 to 169 nm) double-stranded DNA (dsDNA) icosahedral viruses that infect a wide variety of hosts, including teleosts, amphibians, and reptiles (reviewed in references 1 and 2). RVs are increasingly causing diseases and die-offs in various species of natural and captive amphibians around the world and, as such, are possibly involved in the worldwide decline of amphibian populations (4, 7, 11, 14, 15, 46, 48). Frog virus 3 (FV3), the main member and the type species of the RV genus (20), was originally isolated from the native North American leopard frog *Rana pipiens.* FV3 or FV3-like viruses are now found worldwide infecting different amphibian species, making the virus a potentially serious global threat (1, 4).

The frog *Xenopus laevis* has become an instrumental laboratory model to study immunity and pathogenesis of RVs such as FV3 and provides a realistic alternative to field studies of natural populations of endangered amphibians (reviewed in reference 32). The role of the adaptive immune response to RVs is already well established based on studies using FV3 (12, 41). However, although the critical involvement of CD8 T cells (33) and antibodies (12, 24) is now established, very little is yet known about the role of innate immune responses, especially during the early stage of infection. In addition, we have reported some evidence suggesting that macrophage-like cells in the peritoneal cavity of *Xenopus* may harbor FV3 in a fraction of animals that are otherwise asymptomatic (39). These observations laid the groundwork for the present study.

In mammals, macrophages play a key role in virus-host interactions. On the one hand, macrophages are innate immune cell effectors involved in early stages of infection by acting as phagocytic cells that engulf and digest pathogens or infected dying cells in a stimulus-dependent but non-antigen (Ag)-specific manner. In addition, macrophages recruit more phagocytic and effector cells to the area of infection by secreting chemokines such as interleukin-8 (IL-8) and proinflammatory cytokines such as IL-1β and tumor necrosis factor alpha (TNF-α) (reviewed in references 9 and 27). Macrophages are also implicated in adaptive immune responses as professional antigen presenting cells (APCs) that can process viral antigens through major histocompatibility complex class I (MHC-I) and MHC-II presentation pathways to activate CD8 and CD4 T-cell effectors, respectively. On the other hand, viruses can also remain disseminated in macrophages in a quiescent state. Indeed, several viruses (e.g., human immunodeficiency virus and herpes simplex virus 1) infect macrophages and exploit the cells' multiple functions for their own survival. Since macrophages are in constant circulation in the body, they can serve as carriers of the virus to multiple tissues (23, 44).

In the present study we have investigated the response of innate cell effectors in the peritoneal cavity during FV3 infection *in vivo*, as well as their susceptibility to FV3. Our data reveal that peritoneal leukocytes (PLs) may play a dual role in the defense against and pathogenicity of FV3 infection in amphibians.

* Corresponding author. Mailing address: Department of Microbiology and Immunology, University of Rochester Medical Center, Rochester, NY 14642. Phone: (585) 275-1722. Fax: (585) 473-9573. E-mail: Jacques_Robert@urmc.rochester.edu.
† Present address: Vesalius Research Center, Leuven B-3000, Belgium.
▽ Published ahead of print on 3 March 2010.

MATERIALS AND METHODS

Animals, reagents, and FV3 stocks. Two-year-old (about 3 in. long) naïve outbred *Xenopus* adults and monoclonal antibodies (MAbs) specific to FV3 (BG11 [3]) and to *Xenopus* CD5 (2B1 [21]), MHC-II (AM20 [10]), NK cells (1F8 [18]), and IgM (10A9 [19]) were obtained from the *X. laevis* Research Resource for Immunobiology at the University of Rochester Medical Center (http://www.urmc.rochester.edu/smd/mbi/xenopus/index.htm). The frog colony is regularly tested for the presence of FV3 by PCR and is kept free of FV3-asymptomatic carriers. All animals used for primary infection in the experiment presented in the manuscript were either bred from our colony or purchased more than 1 year before the experiments were conducted to minimize as much as possible the risk of a recent primary exposure to FV3 or an FV3-like pathogen. As an additional precaution, we tested serum from a sample of animals used in this study by enzyme-linked immunosorbent assay (ELISA) (24). All sera tested from frogs with a primary infection were negative, whereas anti-FV3 IgY antibodies were detected in sera of frogs with secondary infections (data not shown).

FV3 (*Iridoviridae*) was grown in and purified from baby hamster kidney (BHK-21) cell lines incubated at 30°C during the infection as previously described (12) with the following modification. A single passage of 5 days on BHK-21 cells was done before purification by ultracentrifugation. Viral titers were determined using A6 cells by the 50% endpoint dilution method (37). No marked difference in the viral titer has been observed using BHK-21 cells compared with *Xenopus* A6 cells previously used. Randomized groups of frogs were inoculated by intraperitoneal injection of 1×10^6 to 5×10^6 PFU of FV3 in 300 μl of phosphate-buffered saline (PBS) modified to amphibian osmolarity (APBS) and buffered with sodium bicarbonate at 0.5 g/liter. All animals were handled under strict laboratory regulations and in accordance with the University Committee on Animal Resources ([UCAR] approval number 2007-156), minimizing discomfort at all times.

Flow cytometry. Cells (1×10^6) were incubated for 1 h on ice in 100 μl of undiluted hybridoma supernatant or protein A-purified and biotinylated MAb diluted to 1 μg/ml in APBS–1% bovine serum albumin (BSA). After two washes with APBS–1% BSA, cells were incubated with allophycocyanin-conjugated goat anti-mouse MAb (Accurate JGM136146) diluted 1/300 in staining buffer. A total of 10,000 events were collected and analyzed by FACSCalibur (Becton-Dickinson).

Peritoneal lavage. PLs were isolated by peritoneal lavage with APBS as detailed elsewhere (8). Briefly, each anesthetized 2- to 3-in. frog was injected intraperitoneally (sterile syringe with a $22G1^{1/2}$ gauge needle; one time) with 5 ml of sterile APBS prewarmed to room temperature. The frog was gently massaged, and the solution was drawn into a sterile tube by puncture with a $22G1^{1/2}$ gauge needle. Animals for which less than 4 ml was recovered (out of 5 ml injected) or in which bleeding occurred were not included in the analysis.

Cytospins and Giemsa staining. Cells (100,000 cells in a 200-μl volume) were cytocentrifuged using a Shandon Southern cytospin centrifuge at 500 rpm for 5 min, stained with Giemsa (Fluka 48900), and mounted with Permount (Fisher Scientific). The relative fractions of the different leukocyte types identified according to a *Xenopus* manual (16) were determined in 10 randomly chosen areas (100 by 100 μm; approximately 20 to 40 cells per area) for samples from several individual animals at different time points post-FV3 infection for at least three independent experiments. The average ± standard deviation (SD) of the pooled areas per time point was calculated.

For immunofluorescence studies, cytopsins were rapidly fixed for 30 s in cold 100% acetone (−20°C), dried, and blocked with APBS containing 5% BSA and 5% normal goat serum. Cells were then incubated with anti-FV3 BG11 MAb undiluted supernatant, washed with APBS–1% BSA–0.05% Tween, and incubated with fluorescein isothiocyanate (FITC)-conjugated goat anti-mouse Ig. Preparations were mounted in antifade medium (Molecular Probes Inc., Oregon) and visualized with a Leica DMIRB inverted fluorescence microscope with a cooled charge-coupled device (Cooke) controlled by Image-Pro Plus software (Meida Cybernetics).

TEM. PLs from infected frogs were fixed in osmium tetroxide, processed through a graded series of alcohols, infiltrated into liquid epoxy resin (Epon/Araldite), embedded into molds, and polymerized at 70°C. Thin (70 nm) sections were examined under a Hitachi 7650 transmission electron microscope (TEM) with a Cantega 11-megapixel digital camera and Gatan software for morphometric analysis.

PCR and RT-PCR. RNA was extracted from cells or tissues using Trizol reagent (Invitrogen) and quantified by spectrophotometry. cDNA was synthesized from 0.5 to 1 μg of total mRNA using iScript reverse transcriptase (RT) polymerase. DNA was extracted from the Trizol interphase according to the manufacturer's instructions and quantified. PCR and RT-PCR were done for 30 or 35 cycles. A water-only control (no template) was included in each reaction. For RT-PCR a no-RT control was added to ensure appropriate amplification of cDNA without DNA contamination. All primers spanned at least one intron (Table 1). PCR products were separated on 1% agarose gels and stained with ethidium bromide. Sizes of the PCR products were determined using size standard markers of 1 kb from Invitrogen (Carlsbad, CA).

TABLE 1. Primers and sequences used in this study

Primers name or target	Primer direction and/or sequence[a]
IE gene	F, ATGATCCAAGCCTACCTGTGC
	R, AAATGTCCTAATCTATACACC
Major capsid FV3	F, ATGTCCTTCTGTAACTGGTTCAGG
	R, AAAGACCCGTTTTGCAGCAAAC
Il-1β	F, AACAGAAGATGGCCAAGACTC
	R, ATGCAACCGATTCAAAGC
Arginase 1	F, CTTACAATGAGTAGCCAAGG
	R, GCAGAGAAAATGAGGATTCG
TNF-α	F, GCTCAAGGATAACTCCATCG
	R, AACCAAGTGGCACCTGAATG
LMPX	F, TATCAGTGTCTTCCGCCTCC
	R, CAGCCGTCCTCCTTCATCTG
GAPDH	F, ACCCCTTCATCGACTTGGAC
	R, GGAGCCAGACAGTTTGTAGTG
β2-M consensus-F1[b]	TGACGGTGAATCCTGGAGAC
β2-M consensus-58R	CGATAGCCGTGACAATGAGC
β-Actin-ex2-F1	CCGGTGGTCAAGGTTTACACTG
β-Actin-ex2-R1	TAGAGATCAGTGATTGGATGA

[a] F, forward; R, reverse.
[b] β2-M, β2-microglobulin.

Statistics. A one-way analysis of variance (ANOVA) for independent or correlated samples was performed using an online database available through Vassar Stat, a website for statistical computation (http://faculty.vassar.edu/lowry//anova1u.html). A standard weighted-means analysis was done on five independent samples ($k = 5$) for all samples with n of >5.

RESULTS

Change in numbers and composition of PLs upon FV3 primary and secondary infection. Peritoneal leukocytes (PLs) are a heterogeneous group of cells still poorly characterized in *Xenopus*, especially during immune responses. In addition, there are no antibodies available for *Xenopus* that specifically recognize leukocyte subsets. However, the typical leukocyte types such as neutrophils, basophils, eosinophils, polymorphonuclear (PMN) cells, monocyte and macrophage-like cells, and smaller lymphocytes can be identified as in mammals based on morphology and Giemsa staining patterns (8, 16). Therefore, to determine whether the PL population changes during primary and secondary FV3 infections, we collected PLs by peritoneal lavage at different time points following infection, counted them, and analyzed their composition and morphology on cytospins after Giemsa staining.

First, we noted a slight overall increase in total PLs during FV3 infection already at 1 day postinfection (dpi), but this increase was not statistically significant (Fig. 1). This increase became more marked and statistically significant at 3 dpi (ANOVA, $P < 0.01$) and peaked at 6 dpi, which also corresponds to the maximum T-cell responses observed in the spleen (33). On average, there were two to three times more PLs in frogs at 6 dpi than in control frogs. The total PL number returned to the level of control animals between 9 and 15 dpi, which correlates with the onset of virus clearance in the kidneys (12).

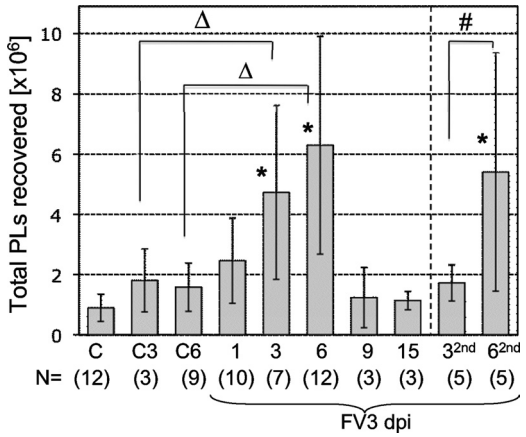

FIG. 1. Total numbers of PLs recovered by lavage during primary and secondary FV3 infection. Averages ± standard deviations from 3 to 4 independent experiments of PLs collected in a volume of approximately 4 to 5 ml of APBS from 2- to 3-in. naïve frogs infected with 1×10^6 to 5×10^6 PFU of FV3 once for 1 to 15 days or at 1 month prior to the experiment and reinfected for 3 (3^{2nd}) and 6 days (6^{2nd}). Control animals were injected with saline vehicle for 3 (C3) or 6 (C6) days or uninjected (C). Statistical significance was determined by ANOVA (*, $P < 0.01$ relative to C; #, $P < 0.01$ between 3^{2nd} and 6^{2nd}; Δ, $P < 0.05$ between C3 and 3; see Materials and Methods for more information) for experimental groups containing more than five animals. Numbers of animals for each group are indicated at the bottom of the graph (N).

As expected, PLs from animals either untreated or injected with amphibian PBS included mainly PMNs, basophils, and eosinophils, as well as a few monocyte/macrophages and lymphocytes without signs of activation. In contrast, PLs from FV3-infected animals revealed an increased abundance of macrophage-like cells identified as large mononuclear cells with purple cytoplasm upon eosin staining (Fig. 2). Most of these peritoneal macrophages displayed an activated phenotype characterized by blastoid (larger) morphology. Macrophage activation was more noticeable at 2 and 3 dpi, with the presence of large numbers of acidic vacuoles (Fig. 2, 3 dpi), more clearly revealed by electron microscopy analysis (Fig. 3A, 2 dpi). These macrophages often formed aggregates. Signs of active phagocytosis were also obvious at 2 and 3 dpi (Fig. 3B). To quantify the accumulation of these macrophage-like cells during FV3 infection, we plotted the average proportion of macrophage-like cells over the total number of PLs in each of 10 randomly selected areas on a slide (100 by 100 μm) (Fig. 4A). In parallel with the total increase of cells in the peritoneal cavity, the relative fraction of macrophages also significantly increased as early as 1 dpi, and they became the major subset, representing on average 40% of PLs at 6 dpi. The other cell subsets did not significantly vary in abundance during FV3 infection, with the exception of lymphocytes, which markedly increased at 6 dpi (data not shown) (Fig. 5).

We have previously shown that during secondary infection, *Xenopus* frogs generate thymus-dependent IgY anti-FV3 antibodies, faster CD8 T-cell responses, and more rapid viral clear-

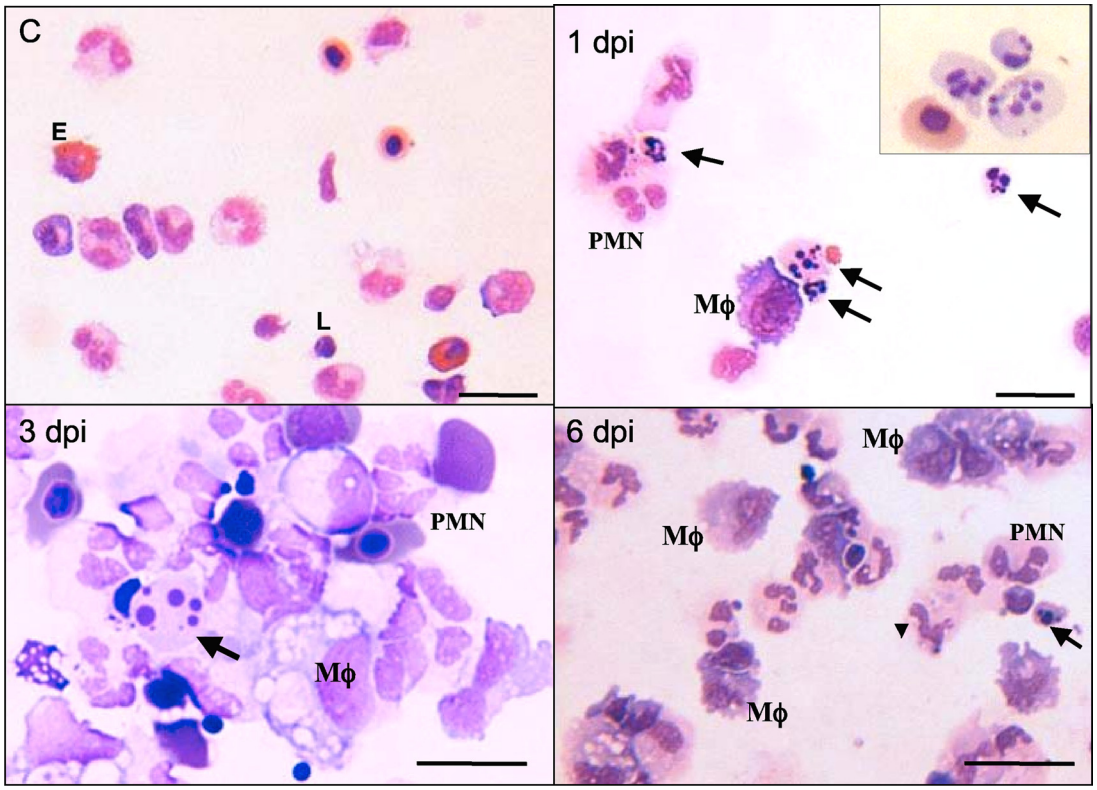

FIG. 2. Peritoneal leukocytes from FV3-infected *Xenopus* adults. Representative images of cytocentrifuged PLs from sham-infected or infected frogs (1×10^6 to 5×10^6 PFU of FV3) for 1, 3, and 6 days. Samples were stained with Giemsa. PMN, polymorphonuclear cells; E, eosinophils, Mϕ, macrophages-like cells; L, lymphocytes. The arrows indicate apoptotic bodies. Scale bar, 100 μm.

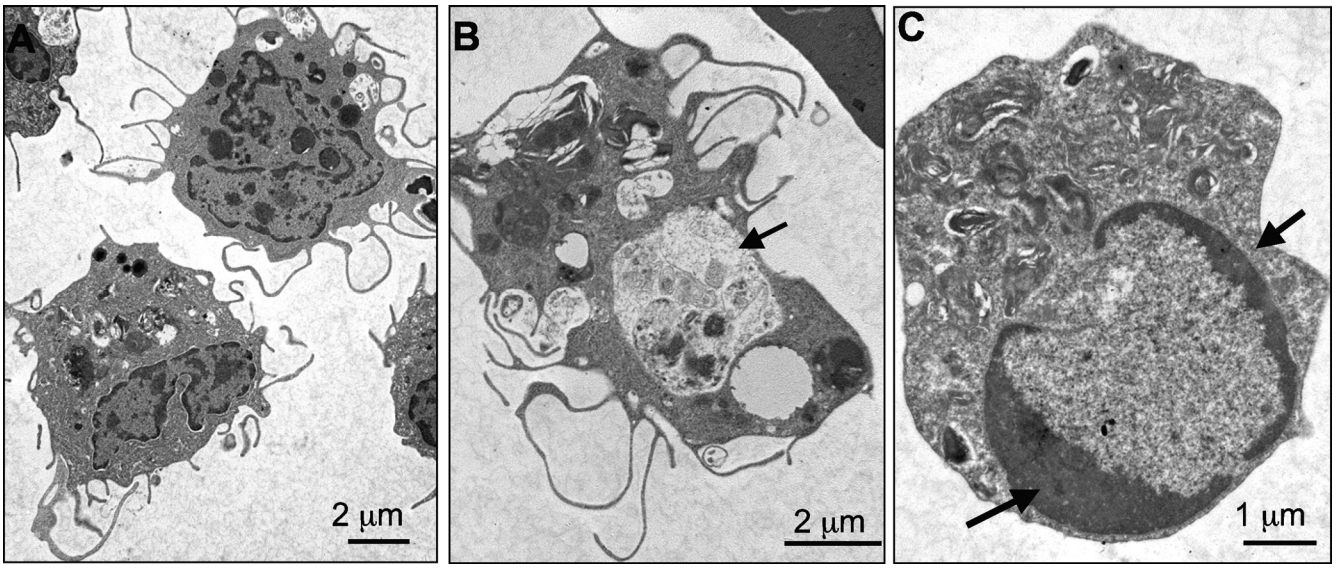

FIG. 3. Electron micrograph of peritoneal macrophage-like cells from FV3-infected *Xenopus* adults. PLs were isolated from frogs at 2 days postinfection with 5×10^6 PFU of FV3, processed, and visualized under a Hitachi 7650 TEM. (A) Two mononucleated macrophage-like cells with multiple pseudopods. (B) A macrophage-like cell with a large phagocytic vacuole (arrow). (C) Apoptotic cells showing heterochromatic condensation (arrows).

ance, all indicative of immunological memory (24, 33). We were therefore interested to determine the effects of a previous exposure to FV3 on PL total numbers and composition during a subsequent infection. PLs were collected from fogs that had been infected 1 month prior to the experiment and reinfected with FV3 for 3 and 6 days. Although the overall changes in PL numbers during primary and secondary infection were similar, some differences were notable. In contrast to primary infection, the increase in total numbers of PLs was significant only at 6 dpi but not at 3 dpi relative to uninfected controls (Fig. 1, 3^{2nd} and 6^{2nd}). In addition, the increase in relative frequency of activated macrophages was statistically significant earlier (3 dpi) during secondary infection than during primary infection (Fig. 4, 3^{2nd} and 6^{2nd}).

These results indicate that FV3 primary infection results in rapid accumulation and activation of macrophages in the peritoneal cavity and that the kinetics of macrophage response but not the increase in total PLs is accelerated during a secondary infection.

Apoptosis of PLs during FV3 infection. FV3 and related viruses are known to be cytolytic, causing apoptosis of infected cell lines *in vitro* and organ failure *in vivo* (2). Interestingly, during our analysis of PLs from FV3-infected animals stained by Giemsa, we noted the presence of a high number of apop-

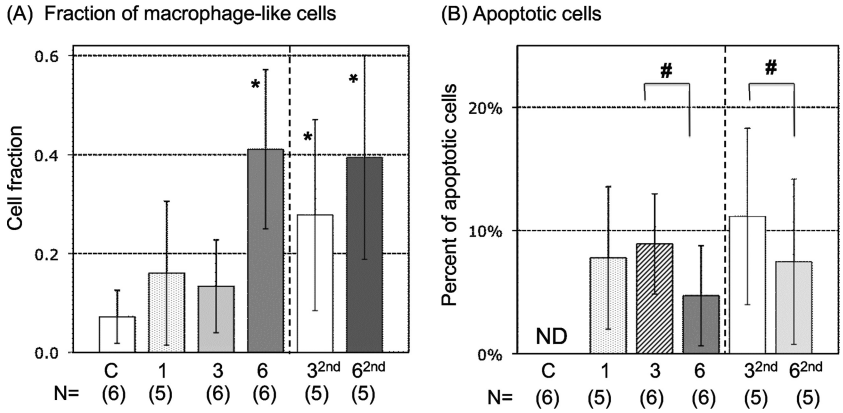

FIG. 4. Relative fraction of macrophage-like cells and apoptotic cells in the peritoneal cavity during primary and secondary FV3 infection. (A) Proportions of macrophage-like cells (expressed as fractions) of the total cells were determined in each of 10 randomly chosen areas of Giemsa-stained cytospin preparations of PLs (approximately 20 to 40 cells per areas). Animals were infected either once for 1, 3, or 6 days or at 1 month prior to the experiment and reinfected for 3 (3^{2nd}) and 6 (6^{2nd}) days. Averages ± SDs of 10 areas for 3 to 6 animals (indicated in parentheses) from three to four independent experiments are shown. *, $P < 0.01$ relative to C at 3^{2nd} or 6^{2nd} dpi and the other groups (ANOVA). (B) Average percentage of apoptotic cells in each of 10 randomly chosen areas of Giemsa-stained cytospin preparations of PLs for 3 to 6 animals from three to four independent experiments. ND, not detected; #, $P < 0.05$ by ANOVA. The control group was not included in the statistical analysis since no apoptotic cells were found.

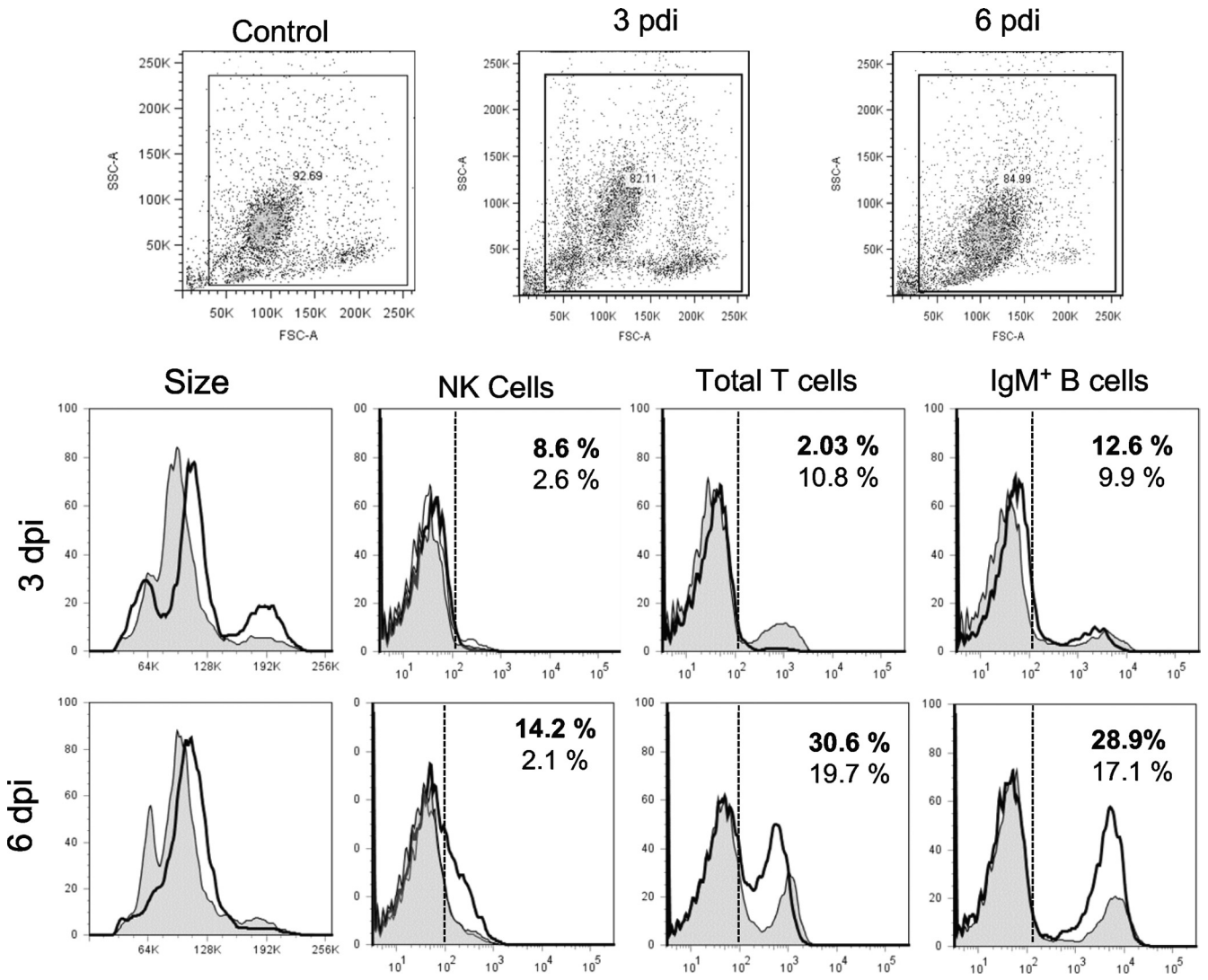

FIG. 5. Lymphocytes and NK cells in PLs of FV3-infected animals. Representative single-color flow cytometry analysis of PLs isolated from uninfected and infected (1×10^6 PFU of FV3) animals at days 1, 3, and 6 postinfection and stained with MAbs specific to *Xenopus* NK cells (1F8), total CD5 T cells, and IgM^+ B cells are shown. Forward and side scatter dot plots (10,000 events collected) with the gates used for the histograms are shown. The percentages of positive cells compared to the isotype control for uninfected (regular fonts) and infected (bold fonts) frogs are indicated. Filled peak, uninfected PLs; solid thick peak, infected PLs; dashed line, limit of signal intensity for 95% of PLs stained with isotype Ab control.

totic cells, identified by pyknotic nuclei indicative of DNA fragmentation (Fig. 2 and 3C). We quantified the occurrence of apoptosis following the same method used for macrophage-like cells by determining, in 10 quadrants, the percentage of apoptotic cells of total cells counted. Whereas no sign of apoptosis was observed in PLs from sham-injected or uninfected animals, significant numbers of apoptotic cells were detected already at 1 dpi, representing on average 8% of cells counted in 10 areas of the cytospin (Fig. 4B). A similar frequency of apoptosis remained at 3 dpi and significantly decreased by 6 dpi, to become rare later on (data not shown). Interestingly, some evidence of phagocytosis of apoptotic bodies was also seen as early as 1 dpi and also at 3 dpi, but their occurrence was too infrequent for quantification (data not shown). During secondary infection, apoptosis was also observed at 3 dpi and, as for primary infection, its frequency significantly decreased at 6 dpi (Fig. 4B, 3^{2nd} and 6^{2nd}).

These data show that some PL cells undergo apoptotic death at early stages of primary and secondary infection by FV3.

Changes in lymphocytes and NK cell population of the peritoneal cavity during FV3 infection. During our microscopy analysis, we observed that cells with lymphocyte morphology became more numerous during the course of an FV3 infection, and we also noted the increased presence of putative NK cells with a granulocyte-like morphology (data not shown). To monitor in more detail the occurrence of lymphocyte subsets and NK cells in the peritoneum during FV3 infection, we stained PLs with available *Xenopus*-specific MAbs recognizing surface markers on NK cells, B cells, and T cells and analyzed them by flow cytometry (representatives of four distinct experiments

TABLE 2. Average percentages of NK, CD5 T, and IgM B cells in the peritoneal cavity of outbred uninfected frogs or frogs at 3 and 6 days post-FV3 infection

Treatment and time point (n)[a]	Cell population (%) in the peritoneal cavity (avg ± SD)[b]		
	NK	T	B
Untreated (10)[c]	2.1 ± 2.0	25.3 ± 13.6	9.3 ± 4.6
Primary infection			
3 dpi (8)	9.8 ± 4.9*	5.2 ± 5.1*	13.3 ± 6.1
6 dpi (9)	10.6 ± 4.5*	21.1 ± 8.7	26.6 ± 4.8*
Secondary infection			
3 dpi (5)	0.6 ± 0.4	9.7 ± 6.7*	11.8 ± 9.7
6 dpi (5)	0.7 ± 0.3	14.5 ± 5.8	29.8 ± 14.4*

[a] n, the total number of animals used.
[b] Data are from four different experiments. *, $P < 0.01$ for infected versus untreated frogs (ANOVA).
[c] In the untreated group, samples from two frogs were pooled (five samples) to get enough cells.

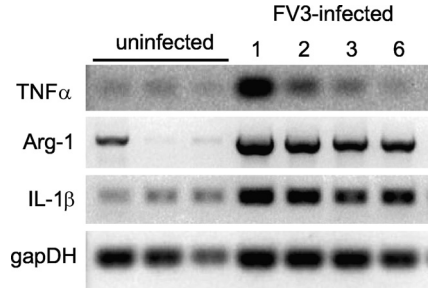

FIG. 6. Expression pattern of proinflammatory genes during FV3 infection. RT-PCR of PLs (1×10^6 cells) isolated from pooled samples of two to three uninfected and infected (1×10^6 PFU FV3) animals at days 1, 2, 3, and 6 postinfection using primers specific for *Xenopus* TNF-α, arginase 1 (Arg-1), IL-1β, and glyceraldehyde-3-phosphate dehydrogenase (GAPDH) as a housekeeping gene control. Except for GAPDH (25 cycles), 30 cycles were used. No signal was detected with RT-negative controls.

are shown in Fig. 5; a summary of all the experiments is in Table 2). A significant increase in the fraction of NK cells identified by the 1F8 MAb (9%) was detected at 3 dpi, which remained noticeable at 6 dpi (10%), whereas very few (~3%) NK cells were detected in sham-infected PLs. On the other hand, there was a marked transitory decrease in total T cells ($CD5^+$) at 3 dpi and a significant increase in IgM-positive (IgM^+) B cells at 6 dpi. A similar transitory decrease in total T cells was also observed during secondary FV3 infection, whereas NK cells were barely detectable (Table 2).

We conclude from these results that in response to primary FV3 infection, NK cells are elicited and migrate into the peritoneal cavity as early as 3 dpi, before the peak of the FV3-elicited T-cell response that occurs at 6 dpi (33).

Change in expression of proinflammatory genes by PLs during FV3 infection. To obtain additional evidence of the initiation of innate immune responses to FV3 infection in the peritoneal cavity, we turned our attention to gene expression, given the absence of relevant antibody (Ab) reagents. We monitored the expression profile of three typical proinflammatory genes for which putative *Xenopus* orthologs have been identified: Il-1β, arginase 1, and TNF-α. Coincident with the increase in the number of PLs and macrophage-like cells at 1 dpi, there was a marked increase in transcripts of the three genes (Fig. 6). This early upregulation of proinflammatory genes was detected in several independent experiments. Some individual variability in the basal level of expression for each gene was observed, presumably due to variations in the health status of individual animals in our colony. The highest level of expression was detected for the three genes at 1 and 2 dpi. The upregulation of TNF-α was more transitory, returning to a basal level at 6 dpi, than that of Il-1β and arginase 1, which still remained highly expressed at 6 dpi.

These data show that FV3 induces a rapid upregulation in *Xenopus* PLs of proinflammatory genes known to be abundantly expressed by macrophages in mammals.

Productive infection of FV3 in PLs. We have previously reported that although the kidney is the main site of FV3 infection, productive FV3 infection in PLs, as determined by viral transcription of the major capsid protein (MCP), is also detectable by RT-PCR from 3 to 12 dpi (39). Given the rapid accumulation of PLs elicited by FV3 infection and their possible involvement in asymptomatic infection, we wanted to study further the kinetics of FV3 infection in PLs and compare it to infection in the kidneys. We isolated both DNA and RNA (DNase-treated) from PLs of frogs infected for different periods of time up to 1 month. We also quantified the infectious virus particles by the 50% tissue culture infective dose ($TCID_{50}$).

In contrast to the kidneys where FV3 is rapidly cleared and becomes undetectable after 9 dpi (33), we detected FV3 viral DNA in PLs by PCR as late as 21 dpi in all the samples tested (Fig. 7); FV3 DNA was not detected in PLs of several frogs at 30 and 60 dpi (data not shown). On the other hand, RT-PCR

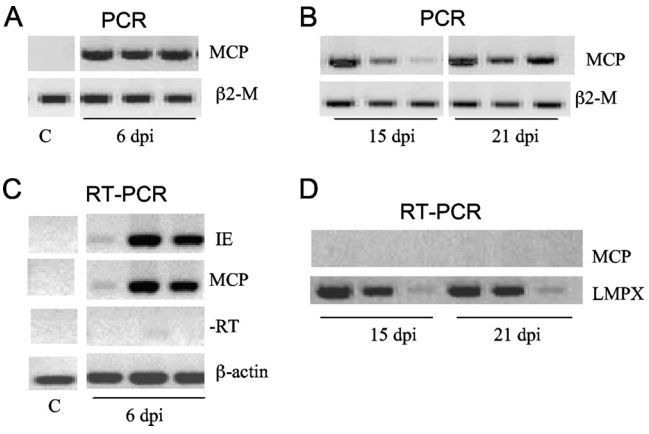

FIG. 7. *In vivo* FV3 infection and transcription in PLs. PCR analysis (35 cycles) was performed on total DNA (0.5 to 1 μg) from PLs isolated from three animals infected for 6 days (A) or for 15 and 21 days (B) with 1×10^6 PFU of FV3 and using primers specific for the FV3 MCP gene and β2-microglobulin (β2-M) as positive controls. RT-PCR analysis was performed on total mRNA (500 ng) isolated from uninfected or infected PLs at 6 days (C) or at 15 and 21 days (D) postinfection using primers for the MCP and IE genes of FV3 and β-actin or LMPX (large multifunctional protease X) as controls for 30 cycles. Data shown are representative of two experiments. −RT, controls lacking reverse transcriptase.

TABLE 3. Detection of viral DNA, viral transcription, and infectious particles in kidney and PL lysates of outbred frogs at different times following FV3 infection

Sample source	Time point (dpi)	Detection of virus by the indicated method[a]		
		PCR[b]	RT-PCR[b]	$TCID_{50}$ (PFU/mg)
Kidney	1	++ (3/3)	+ (3/3)	185
	6	++ (6/6)	+ (6/6)	1,161
	9	+/− (2/3)	+/− (2/3)	320
	14	+/− (1/3)	ND (0/3)	270
PLs	1	++ (3/3)	++ (3/3)	2,161
	3	+ (3/3)	+ (3/3)	+/−[c]
	6	+ (3/3)	+/− (2/3)	ND
	14	+ (3/3)	ND	ND
	20	+ (2/3)	ND	ND
	30	ND (0/6)	ND (0/6)	

[a] ND, not detected.
[b] The numbers in parentheses indicate the number of individuals with detectable signals/the number of individuals tested. ++, high signal intensity; +, medium signal intensity; +/−, weak, barely detectable signal intensity.
[c] Some virus-induced death was observed at low dilutions.

analysis using primers for MCP as well as immediate early (IE) genes of FV3 revealed active viral transcription at 6 dpi, as previously published (33, 39), but not at 15 or 21 dpi. Similar results were obtained in several independent experiments (Table 3). In addition, the poor production of infectious particles by infected PLs is further supported by the low number of PFU obtained by $TCID_{50}$ analysis only at the early stage of infection (1 to 3 dpi), whereas infectious particles were detectable in infected kidneys up to 14 dpi (Table 3).

To get a better idea of the frequency of infected cells in the peritoneal cavity, we used the FV3-specific MAb BG11 (3). To first ensure that BG11 can detect infected PLs, we infected them *in vitro* at a multiplicity of infection (MOI) of between 3 and 1. As shown in Fig. 8, specific signal was detected in a relatively small fraction of cells at 3 dpi (less than 5%). No signal above the auto-fluorescence background was detected with uninfected cells stained with BG11 or with infected cells stained with an isotype control Ab. Interestingly, BG11 also positively stained a small fraction (less than 1%) of PLs harvested from frogs infected for 2 and 3 days. This staining pattern was obtained in several independent experiments, whereas both uninfected cells and isotype controls did not show positive staining patterns. The absence of clear cellular morphology owing to fixation precluded further identification of the cell types stained by BG11. However, analysis by TEM of PLs infected *in vitro* revealed the presence of virus particles in relatively small numbers in the cytoplasm of a small fraction of cells that have a monocytic morphology with phagocytic vesicles and pseudopods typical of macrophages (Fig. 8A, frames c and d).

We conclude from these results that both the kinetics and pathogenesis of FV3 infection of PLs differ from infection in the kidney. Furthermore, the finding that DNA but not transcription is detected in PLs after 2 weeks after infection suggests persistence of a transcriptionally inactive FV3 in innate immune cells, which is consistent with a covert phase of infection.

DISCUSSION

In this study we have addressed the contribution of peritoneal leukocytes in the immune response to FV3 of adult *Xenopus* frogs. Innate immune responses constitute the first line of defense against invading pathogens and can establish host susceptibility to infection. Furthermore, innate immune cells such as macrophages can play a critical part in both innate and adaptive immune responses to viral infections while also often being used as vehicles for viral persistence in a natural host (9, 43). This study is a first attempt at deciphering the dynamic process of host-pathogen interactions in an amphibian host and its natural cognate viral pathogen.

Specifically, our study presents evidence for the first time in amphibians that is consistent with the active and dynamic involvement of macrophage-like cells and NK cells in *Xenopus* adults during early stages of FV3 infection and before the onset of T-cell responses. In addition, our study provides evidence of the particular permissiveness of certain PLs to FV3 infection. Noticeably, the persistence of transcriptionally inactive FV3 genomic DNA in PLs may explain the occurrence of asymptomatic infection and suggests that FV3 is capable of covert infection.

Possible involvement of macrophages and NK cells at early stages of FV3 infection. We have previously shown that during primary FV3 infection, it takes some time for the adult host's adaptive immune response to take place (24) (33). Both T-cell proliferation in the spleen and the infiltration of T cells in the kidney, the main site of infection, become significant only at 6 dpi and onward. Therefore, as in mammals, innate immune cell effectors are likely to play an important role at earlier stages of infection, as well as later on to orchestrate potent host adaptive immune responses. Mononucleated cells with multiple pseudopods typical of macrophage-like cells increase both in numbers and proportion in the peritoneal cavity as early as 1 day postinfection. This strongly suggests a faster response and preponderant role of this cell subset in the innate immune response against FV3. These macrophage-like cells show, especially at 2 and 3 dpi, obvious signs of activation including an increased size (i.e., higher forward scatter), numerous vacuoles, granules, phagocytic bodies, and a propensity to form aggregates. They become the major subset of PLs, constituting almost half of PLs at 6 dpi, the peak of primary FV3 infection. High numbers of PLs containing a majority (50 to 60%) of macrophage-like cells can be elicited by injection of heat-killed *Escherichia coli* and can serve as efficient antigen-presenting cells for minor histocompatibility Ags (40). Preliminary studies suggest that these bacterium-elicited PLs infected *in vitro* with FV3 can induce proliferation of FV3-primed T cells and therefore are likely presenting viral Ags (31). The accumulation of macrophage-like cells before and during the main T-cell response is consistent with their probable involvement as APCs *in vivo*.

The widespread prevalence of FV3 (1) and the fact that we have detected FV3 DNA in kidneys of a fraction of *Xenopus* frogs from various suppliers (39) raise the possibility that some of the frogs used in this study could have been exposed "naturally" to FV3 at some time prior to their being used. As mentioned in Materials and Methods, all animals used in the experiments reported here were either bred from our colony or

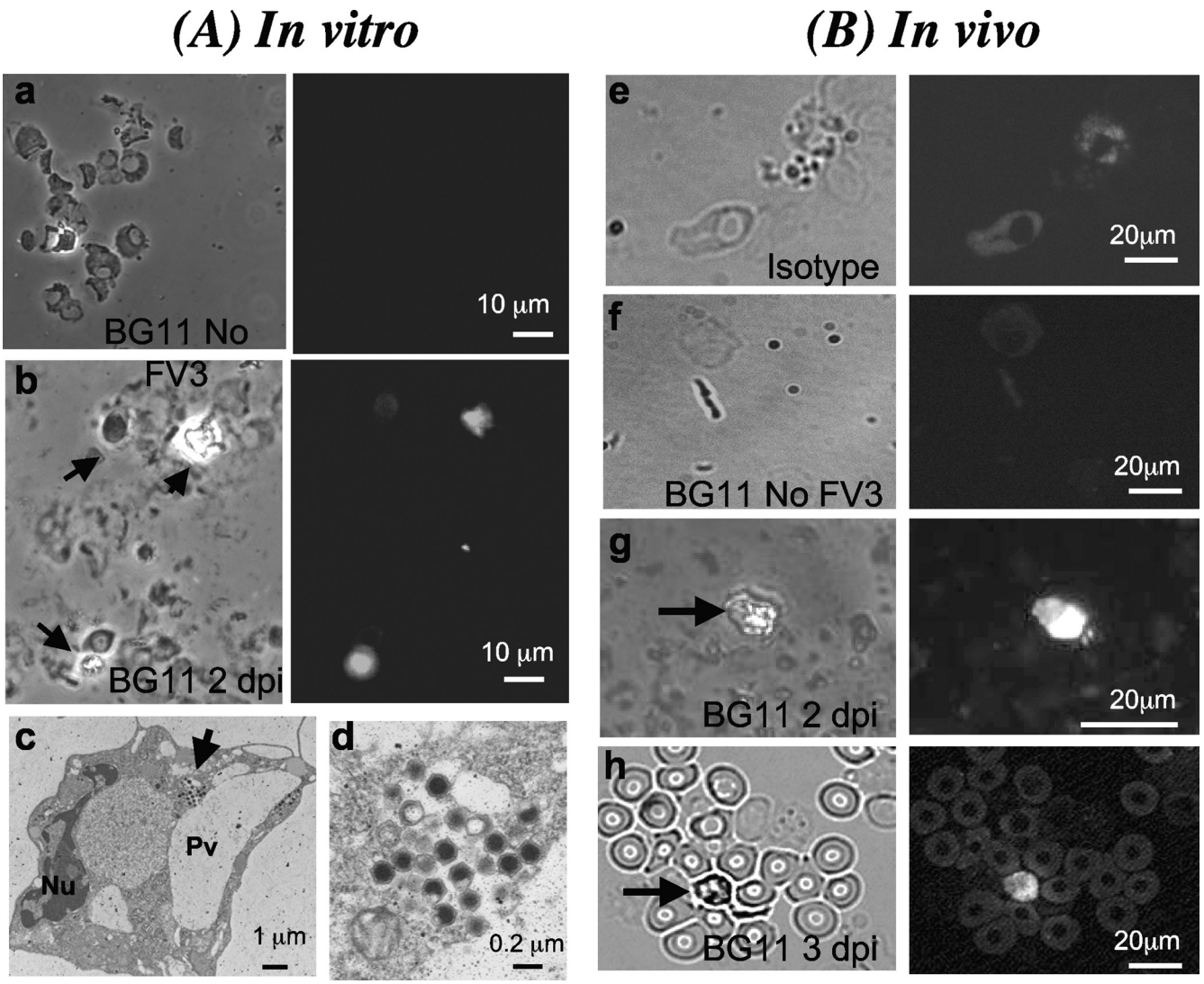

FIG. 8. Immunofluorescence and TEM analysis of PLs infected *in vitro* or *in vivo* with FV3. (A) Representative images of cytocentrifuged PLs obtained from frogs after elicitation with heat-killed bacteria and either mock infected (a) or infected *in vitro* at an MOI of 3 for 2 days (b). Cells were fixed for 30 s in cold (−20°C) acetone, blocked with serum, and incubated with anti-FV3 BG11 MAb undiluted supernatant, followed by an FITC-conjugated goat anti-mouse Ab preadsorbed on *Xenopus* cells. Preparations were visualized with a Leica DMIRB inverted fluorescence microscope using a phase-contrast field (left side of frames a and b) or fluorescence (right side of frames a and b). A TEM view of macrophage-like cells infected *in vitro* is shown in frame c, and the viral capsid in the cytoplasm is shown at higher magnification in frame d. Arrow, viral particle; Nu, nucleus, Pv, phagocytic vesicle. (B) Representative images of cytocentrifuged PLs obtained from sham-infected (e) or infected (5×10^6 PFU of FV3) frogs at 2 days (f) or 3 days (g and h) and processed as described for panel A. Arrows depict positively stained infected cells.

purchased more than a year before the experiments were conducted. Importantly, regular screening for FV3 DNA in the kidneys by PCR in our colony has been negative so far. Tests for serum anti-FV3 antibodies by ELISA in our colony, including animals with primary infections, have also been negative (data not shown). Therefore, we think that one can reasonably consider these animals as immunologically naïve.

The overall similar but distinct increases in total PLs and accumulation of activated macrophages in the peritoneal cavity following a secondary FV3 infection provide further evidence that macrophages are critically involved in a typical host innate immune response during both primary and secondary FV3 infection. The earlier relative increase in the frequency of activated macrophages during secondary infection could be due to the presence of anti-FV3 antibodies and resulting immune complexes although almost nothing is known about macrophage activation by immune complexes in *Xenopus*.

In addition to the rapid cellular response of peritoneal macrophage-like cells initiated by FV3 infection, our study reveals a concomitantly increased expression of several genes involved in innate immune responses that, in mammals, are expressed by activated macrophages. The *Xenopus* IL-1β gene homolog has been characterized and has been shown to be upregulated by lipopolysaccharide (LPS) (47) or by heat-killed bacteria (25). In addition, the functional characterization an IL-1β-like factor produced by stimulated peritoneal leukocytes has been reported in *X. laevis* (42). Therefore, the upregulation of IL-1β induced by FV3 infection is consistent with the activation of

innate immune cell effectors, especially macrophage-like cells. Although in mammals arginase 1 is a cytosolic enzyme, expressed almost exclusively in the liver, it is expressed by activated macrophages in mouse (34) and is increasingly implicated in regulation of alternatively and classically activated macrophages (17, 35). We recently found a putative *Xenopus* homolog of arginase 1 highly upregulated in a microarray analysis of splenocytes during an FV3 infection (H. D. Morales and J. Robert, unpublished data). We confirmed the homology of this gene by sequencing several *X. laevis* expressed sequence tag (EST) clones (GenBank accession number NM_001086948). Phylogenetic analysis of the full-length deduced amino acid coding sequence of this gene unequivocally indicated its homology to arginase 1 (data not shown). The rapid induction of arginase 1 expression by FV3 infection together with the capacity for antigen presentation of PLs provides evolutionary evidence of the critical involvement of this enzyme in the activation process of macrophages. Furthermore, a TNF-α homolog has been characterized and has been shown to activate NF-κB (28). The increased expression of this gene early during FV3 infection, therefore, is consistent with activation of macrophages. TNF-α is a cytokine produced by activated macrophages, T cells, and some other cells. It is a member of a group of cytokines that stimulate the acute-phase reaction in mammals and fish (13, 27). Recent studies in mammals suggest that TNF-α has strong antiviral effects. TNF-α is also involved in antiviral defense in invertebrates (6). In the absence of specific Abs for *Xenopus* macrophages, it is not possible to determine whether these cells are the main producers of TNF-α.

In addition to the possible involvement of macrophages, the present study clearly indicates an increase in NK cells in the peritoneal cavity during primary infection before the onset of the T-cell response in the spleen. NK cells are actively involved in host antiviral defenses in mammals (22). Thus far, however, little is known about the antiviral capabilities of NK cells in amphibians. In *Xenopus*, NK cells recognized by the 1F8 MAb are involved in antitumor responses and mediate cytotoxicity of MHC-negative target cells (18, 36). The increase in the number of 1F8-positive NK cells in PLs within the first week of infection, a time when antiviral innate immune responses are presumed to take place, suggests that NK cells are an important part of the first line of defense against FV3 infection. It remains to be determined if NK cells also infiltrate the kidney early during FV3 infection and, therefore, whether their increased numbers in the peritoneal cavity result from an increase in trafficking. The possible lack of NK cells at 3 and 6 days postsecondary infection would also merit further investigation.

The increase in IgM^+ B cells at 6 dpi is interesting since we have reported that some B cells proliferate in the spleen during FV3 infection (24, 31) and that activated B cells expressing activation-induced cytidine deaminase are present in the periphery (26). The drop in T-cell numbers at 3 dpi, on the other hand, is intriguing. Very little is known about the migration patterns of lymphocytes in *Xenopus*. We have previously reported that total T cells accumulate as early as 3 dpi in the spleen, which in the absence of lymph node is the only draining lymphoid tissue in *Xenopus* (24, 33). Furthermore, splenic T-cell proliferation becomes significant only at 6 dpi, in parallel to the infiltration of CD8 T cells in the kidney, the main site of infection. Therefore, it is possible that the decrease in T cells in the peritoneal cavity at 3 dpi results from their drainage into the spleen, where they become activated. As such, the recovered T-cell population in PLs at 6 dpi may contain an increased fraction of activated T cells. Unfortunately, there are no good markers of T-cell activation in *Xenopus*.

Collectively, our cellular and molecular data strongly suggest that a potent innate immune response mainly involving macrophage-like cells and NK cells is initiated upon primary FV3 infection in parallel with adaptive immune responses already described.

Apoptosis of PLs suggests FV3-mediated cytolysis. We detected apoptotic bodies in PLs within the first days of infection. Apoptotic cells were more numerous within the first and third days of infection and significantly decreased by the sixth day. Pyknotic nuclei are indicative of late apoptosis, suggesting that susceptible cells are quickly eliminated upon FV3 infection and that the clearance by phagocytosis is either overwhelmed or delayed at this stage of infection. Although it can be argued that cells are being eliminated as a result of an active immune response (e.g., cell-mediated cytotoxicity), the fact that many apoptotic cells are seen so early upon infection suggests a direct cytolytic phase of FV3 infection in PLs. Apoptosis induced by FV3 has been reported (2). Indeed, some infected cells detected by immunofluorescence microscopy with BG11 MAb were apoptotic, suggesting that active viral particles within the cells can induce cytotoxicity. Finally, it is still possible that some PL apoptosis induction is related to the release of TNF-α since its expression is enhanced during this period.

It would be interesting to determine whether some PLs are less susceptible to FV3-mediated apoptosis since it is often argued that permissive cells can act as viral reservoirs by allowing virus infection to occur without concomitant cytopathology (44). In addition, phagocytic cells such as macrophages could acquire the virus from the apoptotic cells themselves (38). Indeed, our observation of phagocytosis of apoptotic cells in the same cytospin preparations at 2 and 3 dpi suggests that apoptotic cells are quickly eliminated by the PLs. This is also consistent with the dynamic activity of PLs as they may be further activated by apoptotic stress signals.

Permissiveness of PLs to FV3 infection. Although *Xenopus* adults usually clear FV3 infection within 2 weeks, we have reported the occurrence in animals from various sources of asymptomatic FV3 carriers in which FV3 DNA was detected by PCR without corresponding symptoms of infection (39). Given the involvement of macrophages in several cases of viral quiescence in mammals, we have postulated that macrophage-like cells may also be involved in FV3 covert infection in *Xenopus*. Indeed, various viruses target macrophages in mammals for dissemination in the organism as well as to remain in a quiescent state (38, 44).

We have previously shown that PLs can be infected *in vitro* and that a low level of FV3 infection can be detected in PLs *in vivo* (39). In the present study, we further investigated the fate of FV3 infection in PLs. Interestingly, while we confirmed the ability of FV3 to infect and actively transcribe genes such as MCP and IE during the early phase of infection, the production of infectious particles was very poor compared to that occurring in the kidneys, and it was confined in a small fraction

of PLs. Furthermore, the detection of viral DNA but no viral transcription at later stages of infection (15 and 21 dpi) suggests that FV3 can persist in a transcriptionally inactive form for some time in certain PLs. Although the fixative used for immunofluorescence study did not sufficiently preserve cell morphology to allow us to identify unequivocally which cell types were infected, cells resembling macrophage-like cells were observed. In addition, previous electron microscopy analysis has suggested that in addition to kidney tubular epithelium and, to a lesser extent, hepatocytes from heavily infected frogs, macrophage-like cells in these tissues might also be infected by FV3 (41). Lastly, our TEM analysis of PLs infected *in vitro* has revealed the presence of viral particles in the cytoplasm of cells with macrophage morphology. It will be interesting to determine in future experiments whether FV3 directly infects macrophage-like cells or if FV3 is acquired via phagocytosis of other infected cells. It is important to note that the particular pattern of infection by FV3 on PLs is observed with all frogs infected. In contrast, FV3 DNA is detected in only a fraction (8 to 30%) of asymptomatic animals from different sources and not purposely infected (39). This suggests that the virus has the ability, under certain conditions that remain to be determined, to maintain itself without signs of infection. It is possible, for example, that long-term maintenance of FV3 depends on genetic factors segregating in the population.

Based on our finding that a fraction of *Xenopus* frogs are asymptomatic FV3 carriers, we have proposed that *X. laevis* could act as a viral reservoir, perhaps by maintaining a low level of infection in permissive cells in a covert fashion (39). This suggests that FV3 can remain quiescent in PLs. Sublethal covert (not apparent) infections have been reported for several insect iridoviruses (45). Although these viruses replicate without killing their host, they reduce host fitness. The possibility that RVs, such as FV3, are also capable of covert infections or quiescence would suggest that this phenomenon is a general attribute of iridoviruses.

Covert FV3 could be reactivated by stress signals such as a compromised immune system or subsequent infections. This could explain, for example, the report that RVs are also detected in a captive amphibian colony infected with chytrid fungus, *Batrachochytrium dendrobatidis* (30). It is also possible that hormonal fluctuations, such as those induced by environmental toxins, could reactivate previously asymptomatic infections (5, 29). All of these possibilities need further testing, and with the use of PLs as a diagnostic tool in wild animals, the effect that emerging infectious diseases have on amphibian populations can be further investigated (32).

ACKNOWLEDGMENTS

The expert animal husbandry provided by Tina Martin and David Albright is gratefully appreciated. We thank Karen L. de Mesy Bentley for her technical assistance in electron microscopy analysis, as well as Tanya Cruz Luna and Pamela McPherson for their significant technical contribution. We also thank Ana Goyos and Hristina Nedelkovska, as well as Nicholas Cohen, for their critical reviews of the manuscript.

This research was supported by grants T32-AI-07285 (H.D.M.) and R24-AI-059830-1 from the NIH and grant MCB-0136536 from the NSF.

REFERENCES

1. **Chinchar, V. G.** 2002. Ranaviruses (family *Iridoviridae*): emerging cold-blooded killers. Arch. Virol. **147:**447–470.
2. **Chinchar, V. G., L. Bryan, J. Wang, S. Long, and G. D. Chinchar.** 2003. Induction of apoptosis in frog virus 3-infected cells. Virology **306:**303–312.
3. **Chinchar, V. G., D. W. Metzger, A. Granoff, and R. Goorha.** 1984. Localization of frog virus 3 proteins using monoclonal antibodies. Virology **137:**211–216.
4. **Cunningham, A. A., A. D. Hyatt, P. Russell, and P. M. Bennett.** 2007. Emerging epidemic diseases of frogs in Britain are dependent on the source of ranavirus agent and the route of exposure. Epidemiol. Infect. **135:**1200–1212.
5. **Daszak, P., L. Berger, A. A. Cunningham, A. D. Hyatt, D. E. Green, and R. Speare.** 1999. Emerging infectious diseases and amphibian population declines. Emerg. Infect. Dis. **5:**735–748.
6. **De Zoysa, M., S. Jung, and J. Lee.** 2009. First molluscan TNF-alpha homologue of the TNF superfamily in disk abalone: molecular characterization and expression analysis. Fish Shellfish Immunol. **26:**625–631.
7. **Duffus, A. L., B. D. Pauli, K. Wozney, C. R. Brunetti, and M. Berrill.** 2008. Frog virus 3-like infections in aquatic amphibian communities. J. Wildl. Dis. **44:**109–120.
8. **Du Pasquier, L., M. F. Flajnik, C. Guiet, and E. Hsu.** 1985. Methods used to study the immune system of *Xenopus* (Amphibia, Anura). Immunol. Methods **3:**425–465.
9. **Ellermann-Eriksen, S.** 2005. Macrophages and cytokines in the early defence against herpes simplex virus. Virol. J. **2:**59.
10. **Flajnik, M. F., S. Ferrone, N. Cohen, and L. Du Pasquier.** 1990. Evolution of the MHC: antigenicity and unusual tissue distribution of *Xenopus* (frog) class II molecules. Mol. Immunol. **27:**451–462.
11. **Fox, S. F., A. L. Greer, R. Torres-Cervantes, and J. P. Collins.** 2006. First case of ranavirus-associated morbidity and mortality in natural populations of the South American frog *Atelognathus patagonicus*. Dis. Aquat. Organ. **72:**87–92.
12. **Gantress, J., G. D. Maniero, N. Cohen, and J. Robert.** 2003. Development and characterization of a model system to study amphibian immune responses to iridoviruses. Virology **311:**254–262.
13. **Grayfer, L., and M. Belosevic.** 2009. Molecular characterization of tumor necrosis factor receptors 1 and 2 of the goldfish (Carassius aurutus L.). Mol. Immunol. **46:**2190–2199.
14. **Green, D. E., K. A. Converse, and A. K. Schrader.** 2002. Epizootiology of sixty-four amphibian morbidity and mortality events in the U.S.A., 1996–2001. Ann. N. Y. Acad. Sci. **969:**323–339.
15. **Greer, A. L., M. Berrill, and P. J. Wilson.** 2005. Five amphibian mortality events associated with ranavirus infection in south central Ontario, Canada. Dis. Aquat. Organ. **67:**9–14.
16. **Hadji-Azimi, I., V. Coosemans, and C. Canicatti.** 1987. Atlas of adult *Xenopus laevis laevis* hematology. Dev. Comp. Immunol. **11:**807–874.
17. **Hesse, M., M. Modolell, A. C. La Flamme, M. Schito, J. M. Fuentes, A. W. Cheever, E. J. Pearce, and T. A. Wynn.** 2001. Differential regulation of nitric oxide synthase-2 and arginase-1 by type 1/type 2 cytokines in vivo: granulomatous pathology is shaped by the pattern of L-arginine metabolism. J. Immunol. **167:**6533–6544.
18. **Horton, T. L., R. Minter, R. Stewart, P. Ritchie, M. D. Watson, and J. D. Horton.** 2000. *Xenopus* NK cells identified by novel monoclonal antibodies. Eur. J. Immunol. **30:**604–613.
19. **Hsu, E., and L. Du Pasquier.** 1984. Studies on *Xenopus* immunoglobulins using monoclonal antibodies. Mol. Immunol. **21:**257–270.
20. **Hyatt, A. D., A. R. Gould, Z. Zupanovic, A. A. Cunningham, S. Hengstberger, R. J. Whittington, J. Kattenbelt, and B. E. Coupar.** 2000. Comparative studies of piscine and amphibian iridoviruses. Arch. Virol. **145:**301–331.
21. **Jurgens, J. B., L. A. Gartland, L. Du Pasquier, J. D. Horton, T. W. Gobel, and M. D. Cooper.** 1995. Identification of a candidate CD5 homologue in the amphibian *Xenopus laevis*. J. Immunol. **155:**4218–4223.
22. **Lee, S. H., T. Miyagi, and C. A. Biron.** 2007. Keeping NK cells in highly regulated antiviral warfare. Trends Immunol. **28:**252–259.
23. **Lin, C. L., A. K. Sewell, G. F. Gao, K. T. Whelan, R. E. Phillips, and J. M. Austyn.** 2000. Macrophage-tropic HIV induces and exploits dendritic cell chemotaxis. J. Exp. Med. **192:**587–594.
24. **Maniero, G. D., H. Morales, J. Gantress, and J. Robert.** 2006. Generation of a long-lasting, protective, and neutralizing antibody response to the ranavirus FV3 by the frog *Xenopus*. Dev. Comp. Immunol. **30:**649–657.
25. **Marr, S., A. Goyos, J. Gantress, G. D. Maniero, and J. Robert.** 2005. CD91 up-regulates upon immune stimulation in *Xenopus* adult but not larval peritoneal leukocytes. Immunogenetics **56:**735–742.
26. **Marr, S., H. Morales, A. Bottaro, M. Cooper, M. Flajnik, and J. Robert.** 2007. Localization and differential expression of activation-induced cytidine deaminase in the amphibian *Xenopus* upon antigen stimulation and during early development. J. Immunol. **179:**6783–6789.
27. **Martinez, F. O., L. Helming, and S. Gordon.** 2009. Alternative activation of macrophages: an immunologic functional perspective. Annu. Rev. Immunol. **27:**451–483.
28. **Mawaribuchi, S., K. Tamura, S. Okano, S. Takayama, Y. Yaoita, T. Shiba, N. Takamatsu, and M. Ito.** 2008. Tumor necrosis factor-alpha attenuates thyroid hormone-induced apoptosis in vascular endothelial cell line XLgoo established from *Xenopus* tadpole tails. Endocrinology **149:**3379–3389.

29. **Mendelson, J. R., III, E. D. Brodie, Jr., J. H. Malone, M. E. Acevedo, M. A. Baker, N. J. Smatresk, and J. A. Campbell.** 2004. Factors associated with the catastrophic decline of a cloudforest frog fauna in Guatemala. Rev. Biol. Trop. **52:**991–1000.
30. **Miller, D. L., S. Rajeev, M. Brookins, J. Cook, L. Whittington, and C. A. Baldwin.** 2008. Concurrent infection with ranavirus, *Batrachochytrium dendrobatidis*, and *Aeromonas* in a captive anuran colony. J. Zoo Wildl. Med. **39:**445–449.
31. **Morales, H., and J. Robert.** 2008. In vivo and in vitro techniques for comparative study of antiviral T-cell responses in the amphibian *Xenopus*. Biol. Proced. Online **10:**1–8.
32. **Morales, H., and J. Robert.** Relations between the state of immune defenses and the increased prevalence of viral and fungal infectious diseases in wild and cultured amphibian populations, p. 407–424. *In* J. B. Aronoff (ed.), Nature conservation: global, environmental, and economic issues, in press. Nova Science Publishers, Inc., New York, NY.
33. **Morales, H. D., and J. Robert.** 2007. Characterization of primary and memory CD8 T-cell responses against ranavirus (FV3) in Xenopus laevis. J. Virol. **81:**2240–2248.
34. **Munder, M., K. Eichmann, J. M. Moran, F. Centeno, G. Soler, and M. Modolell.** 1999. Th1/Th2-regulated expression of arginase isoforms in murine macrophages and dendritic cells. J. Immunol. **163:**3771–3777.
35. **Pesce, J. T., T. R. Ramalingam, M. M. Mentink-Kane, M. S. Wilson, K. C. El Kasmi, A. M. Smith, R. W. Thompson, A. W. Cheever, P. J. Murray, and T. A. Wynn.** 2009. Arginase-1-expressing macrophages suppress Th2 cytokine-driven inflammation and fibrosis. PLoS Pathog. **5:**e1000371.
36. **Rau, L., J. Gantress, A. Bell, R. Stewart, T. Horton, N. Cohen, J. Horton, and J. Robert.** 2002. Identification and characterization of *Xenopus* $CD8^+$ T cells expressing an NK cell-associated molecule. Eur. J. Immunol. **32:**1574–1583.
37. **Reed, L., and H. Muench.** 1983. A simple method of estimating fifty percent endpoints. Am. J. Hyg. **27:**493–497.
38. **Rigden, R. C., C. P. Carrasco, A. Summerfield, and M. C. KC.** 2002. Macrophage phagocytosis of foot-and-mouth disease virus may create infectious carriers. Immunology **106:**537–548.
39. **Robert, J., L. Abramowitz, J. Gantress, and H. D. Morales.** 2007. *Xenopus laevis*: a possible vector of Ranavirus infection? J. Wildl. Dis. **43:**645–652.
40. **Robert, J., A. Goyos, and H. Nedelkovska.** 2009. Xenopus, a unique comparative model to explore the role of certain heat shock proteins and nonclassical MHC class Ib gene products in immune surveillance. Immunol. Res. **45:**114–122.
41. **Robert, J., H. Morales, W. Buck, N. Cohen, S. Marr, and J. Gantress.** 2005. Adaptive immunity and histopathology in frog virus 3-infected *Xenopus*. Virology **332:**667–675.
42. **Watkins, D., S. C. Parsons, and N. Cohen.** 1987. A factor with interleukin-1-like activity is produced by peritoneal cells from the frog, *Xenopus laevis*. Immunology **62:**669–673.
43. **Way, S. J., B. A. Lidbury, and J. L. Banyer.** 2002. Persistent Ross River virus infection of murine macrophages: an in vitro model for the study of viral relapse and immune modulation during long-term infection. Virology **301:**281–292.
44. **Weck, K. E., S. S. Kim, H. I. Virgin, and S. H. Speck.** 1999. Macrophages are the major reservoir of latent murine gammaherpesvirus 68 in peritoneal cells. J. Virol. **73:**3273–3283.
45. **Williams, T., V. Barbosa-Solomieu, and V. G. Chinchar.** 2005. A decade of advances in iridovirus research. Adv. Virus Res. **65:**173–248.
46. **Zhan, Q. Y., F. Xiao, Z. Q. Li, J. F. Gui, J. Mao, and V. G. Chinchar.** 2001. Characterization of an iridovirus from the cultured pig frog Rana grylio with lethal syndrome. Dis. Aquat. Organ. **48:**27–36.
47. **Zou, J., S. Bird, R. Minter, J. Horton, C. Cunningham, and C. J. Secombes.** 2000. Molecular cloning of the gene for interleukin-1β from *Xenopus laevis* and analysis of expression in vivo and in vitro. Immunogenetics **51:**332–338.
48. **Zupanovic, Z., G. Lopez, A. D. Hyatt, B. Green, G. Bartran, H. Parkes, R. J. Whittington, and R. Speare.** 1998. Giant toads Bufo marinus in Australia and Venezuela have antibodies against "ranaviruses." Dis. Aquat. Organ. **32:**1–8.